



Published in final edited form as:

Toxicol Appl Pharmacol. 2008 October 15; 232(2): 236–243. doi:10.1016/j.taap.2008.06.022.

Metabolomic profiling of a modified alcohol liquid diet model for liver injury in the mouse uncovers new markers of disease

Blair U. Bradford¹, Thomas M. O'Connell², Jun Han¹, Oksana Kosyk¹, Svitlana Shymonyak¹, Pamela K. Ross¹, Jason Winnike², Hiroshi Kono³, and Ivan Rusyn¹

¹Department of Environmental Sciences & Engineering, University of North Carolina at Chapel Hill, Chapel Hill, NC, USA

²Division of Molecular Pharmaceutics, School of Pharmacy, University of North Carolina at Chapel Hill, Chapel Hill, NC, USA

³First Department of Surgery, University of Yamanashi, Yamanashi, Japan

Abstract

Metabolomic evaluation of urine and liver was conducted to assess the biochemical changes that occur as a result of alcohol-induced liver injury. Male C57BL/6J mice were fed an isocaloric control- or alcohol-containing liquid diet with 35% of calories from corn oil, 18% protein and 47% carbohydrate/alcohol for up to 36 days *ad libitum*. Alcohol treatment was initiated at 7 g/kg/day and gradually reached a final dose of 21 g/kg/day. Urine samples were collected at 22, 30 and 36 days and in additional treatment groups, liver and serum samples were harvested at 28 days. Steatohepatitis was induced in the alcohol-fed group since a 5-fold increase in serum alanine aminotransferase activity, a 6-fold increase in liver injury score (necrosis, inflammation and steatosis) and an increase in lipid peroxidation in liver were observed. Liver and urine samples were analyzed by nuclear magnetic resonance spectroscopy and electrospray infusion/Fourier transform ion cyclotron resonance-mass spectrometry. In livers of alcohol-treated mice the following changes were noted. Hypoxia and glycolysis were activated as evidenced by elevated levels of alanine and lactate. Tyrosine, which is required for L-DOPA and dopamine as well as thyroid hormones, was elevated possibly reflecting alterations of basal metabolism by alcohol. A 4-fold increase in the prostacyclin inhibitor 7,10,13,16-docosatetraenoic acid, a molecule important for regulation of platelet formation and blood clotting, may explain why chronic drinking causes serious bleeding problems. Metabolomic analysis of the urine revealed that alcohol treatment leads to decreased excretion of taurine, a metabolite of glutathione, and an increase in lactate, n-acetylglutamine and n-acetylglycine. Changes in the latter two metabolites suggest an inhibition of the kidney enzyme aminoacylase I and may be useful as markers for alcohol consumption.

Keywords

alcohol; liver; mouse; metabolomics

Send all correspondence to: Dr. Ivan Rusyn, 0031 Michael Hooker Research Center, CB #7431, Department of Environmental Sciences and Engineering, University of North Carolina at Chapel Hill, Chapel Hill, NC 27599-7431, Phone# (919) 843-2596, FAX# (919) 843-2596 E-mail: iir@unc.edu.

Publisher's Disclaimer: This is a PDF file of an unedited manuscript that has been accepted for publication. As a service to our customers we are providing this early version of the manuscript. The manuscript will undergo copyediting, typesetting, and review of the resulting proof before it is published in its final citable form. Please note that during the production process errors may be discovered which could affect the content, and all legal disclaimers that apply to the journal pertain.

Introduction

In North America, liver disease due to alcohol consumption is an important cause of death in adults, although its pathogenesis remains largely unknown. The disease process is characterized by early steatosis, inflammation, and necrosis (often called alcoholic steatohepatitis). In some individuals who abuse alcoholic beverages, liver disease progresses to fibrosis and cirrhosis, which significantly impairs liver function, and can ultimately lead to the development of hepatocellular carcinoma (Purohit et al., 2005; Purohit and Brenner, 2006).

Much has been learned about the molecular mechanisms of liver damage by alcohol from experiments in model organisms, especially rats and knockout mice (Thurman, 1998). The Lieber-DeCarli liquid diets contain carbohydrates (11% of calories), protein (18%), fat (35%), and alcohol or maltose dextrin (36%) (Lieber and DeCarli, 1982). The diet is administered to animals *ad libitum* and, together with its low-fat and high-protein modifications, is readily available commercially which makes this model easy to use. While animals on Lieber-DeCarli diets have circulating blood alcohol levels around 200 mg/dl after as early as one week of feeding (Sibley and Jerrells, 2000) and liver steatosis develops, the injury has not been reported to progress much farther in mice. Thus, the Lieber-DeCarli model provides only a limited resource for studies of alcohol-related liver disease.

The continuous intragastric enteral alcohol feeding protocol in the rat, known as Tsukamoto-French model (Tsukamoto et al., 1984), was a major development in alcohol-induced liver injury research. While this method requires animal surgery and is very labor intensive, it produces liver injury that is consistent with the human disease starting with steatosis, progressing to steato-hepatitis and achieving fibrosis after 3 months of exposure in the rat (Tsukamoto et al., 1990). This force feeding (through an intragastric cannula) protocol was also adapted to the mouse which allowed mechanistic studies in genetically engineered animals (Kono et al., 1999; Yin et al., 1999). Interestingly, alcohol must be delivered in a high fat corn oil-based diet in order to facilitate the progression of the liver injury in rodents (Nanji et al., 1989). Recent studies have also implicated fish oil as a source of potentiation of injury in female as compared to males rats using a liquid diet which is formulated similarly to the enteral model (Donohue et al., 2007).

The advantages of the enteral model over liquid diet models include continuous delivery of alcohol 24 hours a day which simulates binge drinking, robustness of the liver injury phenotype, and a characteristic cycling in urine alcohol concentrations due to diurnal variation in basal metabolism and hormones. The criticisms of the Tsukamoto-French model have been that it is labor intensive, does not follow a normal nocturnal feeding pattern for rodents, and that the diet is not nutritionally adequate for induction of cytochrome P450 to the same extent as a standard Lieber-DeCarli liquid diet (Ronis et al., 1991), although it has been reported recently that P450s are well induced in mice and rats after enteral alcohol treatment (Isayama et al., 2003; Bradford et al., 2005). Since the 'success' of each model is assessed largely by its effectiveness to produce liver damage as the key endpoint, the development of an easy-to-use model that produces significant liver injury is desired.

Recently, it was shown that by feeding rats a high fat corn oil-based modified Lieber-DeCarli diet together with daily administration of a large dose of alcohol by gavage produced liver injury similar to that shown by the Tsukamoto-French model after 8 weeks of treatment (Enomoto et al., 1999). Similar experiments were not successful in the mouse (N. Enomoto, personal communication), possibly due to the stress of daily gavage. Thus, this study was conducted to determine if by using corn oil as the source of fat in the standard Lieber-DeCarli liquid diet it is possible to achieve a liver injury phenotype more similar to human disease. We show that this protocol results in the development of steatohepatitis comparable to that in the

Tsukamoto-French model. Furthermore, we utilized metabolomic analysis of the urine and liver extracts to assess the biochemical and molecular changes of the disease progression toward alcohol-induced liver injury.

Methods

Animals and Treatments

Male C57Bl/6J mice 6–8 weeks of age were fed *ad lib* a modified Lieber-DeCarli liquid diet (Cat #710270; Dyets, Inc; Bethlehem PA) for up to 36 days. The diet contained 35% of calories from fat (corn oil), 12% from carbohydrate, 18% from protein, and 35% from ethyl alcohol (alcohol group) or isocaloric maltose dextrin (control group). Alcohol-containing diet was diluted with control diet to gradually increase acclimation to alcohol. Alcohol treatment was initiated with a dose of 7 g/kg/day and gradually increased to 21 g/kg/day by day 13. Urine was collected on day 22, 30 and 36 by housing mice in individual metabolic cages for 24 hours. Separate groups of mice were treated in an identical manner and animals were sacrificed at 28 days for collection of serum and liver. Sections of liver were evaluated for several histological indices. Scoring of liver injury was performed using the method developed by Nanji (Nanji et al., 1989). Additional liver sections were stained with Oil Red O and PAS reagent, which are specific for fat and glycogen, respectively, and were quantified using image analysis software (BioQuant Image Analysis Corp, Nashville, TN). Staining for 4-hydroxynonenal was performed using a 1:500 dilution of anti-4HNE antibody (Alpha Diagnostics, San Antonio, TX; HNE11-S) for 1 hr and counterstained using the DAKO Envision System- HRP (DAKO Carpinteria, CA ; K1392) following blocking of non specific binding with 1:10 dilution of normal goat serum for 30 minutes. Serum samples were analyzed colorimetrically for a common marker of liver injury alanine aminotransferase (ALT) and urine for creatinine levels. Urine osmolarity was determined using an osmometer (model 5004, Precision Systems, Natick, MA). Urine samples were analyzed by nuclear magnetic resonance (NMR) and liver by NMR and electrospray infusion/ Fourier transform ion cyclotron resonance-mass spectrometry (ESI/FITCR- MS).

Liver extraction and analysis by ESI/FTICR-MS and NMR

A 50 mg sample of frozen liver from each mouse was homogenized in 500 μ l of dH₂O using a TissueLyser (Qiagen, Valencia, CA) for 5 min at 25 Hz. Next, 100 μ l of tissue homogenate was added to 100 μ l dH₂O and 1000 μ l methanol which was vortexed then sonicated in icy water for 1 min \times 3. The samples were placed at -20°C for at least 2 hr followed by centrifugation at 12,000 rpm at 4°C for 10 min. An aliquot of 600 μ l of the supernatants were transferred to a 2 ml tube and 400 μ l dH₂O and 500 μ l chloroform was added and vortexed. The samples were cooled to -20°C for 2 hr and centrifuged at 5000 rpm for 15 min 4°C to separate an upper (aqueous) phase and a lower (organic) phase. 800 μ l of the upper phase and 400 μ l of the lower phase were carefully transferred to two respective 1.5-mL tubes.

The organic phase was dried and reconstituted in 800 μ l 80% methanol and were spiked with 200 μ l of internal standard solution (haloperidol 0.2 μ g/mL, verapamil 0.1 μ g/mL and reserpine 0.1 μ g/mL, freshly made in methanol/ dH₂O, 80:20, v/v). Samples were acidified using 0.1% formic acid and then directly infused into a Bruker 12-Tesla FTICR-MS instrument (Bruker, Billerica, MA) in positive electrospray ionization (ESI) mode at a flow rate of 2 μ l/min. Duplicate mass spectra were acquired within 100–900 m/z using a total of accumulation time of 0.5 s, 100 scans per mass spectrum in approximately 3 min.

The liver extracts from the aqueous phase were dried down using a speed-vac and re-suspended in 7 μ l of dH₂O containing TSP as described for the urine samples. The liver extracts were analyzed on the Varian Inova 400MHz NMR using a 5 μ l CapNMR probe (Protasis Magnetic

Resonance Microsensors, Urbana-Champaign, IL). The sample was introduced into the probe using manual syringe injection connected to capillary tubing. The spectra were acquired with 256 transients with a sweep width of 5000Hz. The pulse sequence included a 500 ms solvent pre-saturation period, 45° excitation pulse and a 3.3 second acquisition time.

Urine analysis by NMR

Frozen urine samples were allowed to thaw at room temperature. Aliquots of 540 µl of urine were analyzed following the addition of 60 µl of a dH₂O solution containing 5 mM trimethylsilylpropionate as a reference for concentration and chemical shift. The solutions were transferred to 5 mm NMR tubes. NMR spectra on the mouse urine samples were acquired on a Varian Inova 400 MHz using a 5 mm pulsed field gradient, inverse detection probe (Varian, Inc., Palo Alto, CA). The spectra were acquired with 1024 transients and a sweep width of 4650 Hz. The pulse sequence included a 4 second solvent pre-saturation period and a 2.6 second acquisition time. A 45° excitation pulse was used to provide quantitative results.

NMR Metabolite Identification

The data were processed using ACD software version 9 (Advanced Chemistry Development, Toronto, Canada). A 0.1Hz exponential line broadening was applied to the data. The spectra were phased, baseline corrected and integrated using the ACD intelligent binning algorithm. The regions from 0.5 to 4.7 ppm and 4.9 to 9.0 were included in the integration. The regions below 0.5 and above 9.0 contained only noise and the region from 4.7 to 4.9 contained the residual solvent peak. The data were normalized by setting the sum of all integrals equal to 1000 for each spectrum. To account for the presence of alcohol and ethyl glucuronide in the samples from alcohol treated mice, the spectra were renormalized after removal of the bins containing these peaks. Metabolite identification was made using the Chenomx NMR suite version 4.5 metabolite data base (Chenomx Inc, Edmonton, Canada). Confirmation of assignments was aided by two-dimensional ¹H-¹³C gHSQC and gHMBC experiments on selected samples.

ESI/FTICR-MS Metabolite Identification

Raw mass spectra were initially batch processed using a custom VBA script within Bruker's DataAnalysis™ software to pick up monoisotopic ion peaks based on variable isotopic distribution patterns (Han et al., 2008). The resulting monoisotopic mass lists together with their ion intensities and charge states from each spectrum were further processed with another custom software program (Han et al., 2008) written with LabView™ development software to do internal mass calibration with the mass calibration standards (haloperidol, verapamil, reserpine and a known endogenous metabolite, phosphocholine at m/z 184.0733). The ion intensity of each picked monoisotopic peaks on a spectrum were normalized to the total ion intensity of all the picked monoisotopic ion peaks. The resulting mass lists were then filtered to recognize sodium (+22.9892) and potassium (+38.9632) adduct ions and binned to a unique neutral mass. The total intensity from the protonated, sodiated, and potassiated ions of the same metabolite was summed up. Duplicate measurements of each sample were compared to verify correlation (i.e., to ensure that there were no instrumental problems affecting signal acquisition or instrument calibration during that particular run). Masses observed in the set of correlated replicates were combined into a single biological replicate by averaging intensities from masses that matched within a selectable mass accuracy (typically 2 ppm). Biological replicates from multiple animals were then aligned to yield a list of masses observed. Aligned mass lists from sets of control and alcohol-treated animals were then combined, keeping all mass values regardless of their occurrence across the set. For metabolite assignment, chemical molecular formulae incorporating unlimited number of C, H, N, O, and a maximum of two S, three P, one Na and one potassium) were generated based on accurate masses using the Generate

Molecular Formula tool with DataAnalysis™ software. The Human Metabolome database (<http://www.hmdb.ca/>) and Lipid Maps Database (www.lipidmaps.org/data/structure/text_search.php) were used to search potential matching metabolites consistent with the measured mass with 1 ppm.

Statistical Analysis

The statistical analyses on NMR data were performed using SimcaP+ v.11.5 software (Umetrics, Umea, Sweden). Pareto scaling was applied to the NMR integration data prior to principal component analysis and orthogonal partial least squares analysis. Markers of liver injury were assessed using student's t-test.

Results

Modified Lieber-DeCarli diet produces steato-hepatitis in mice

Feeding of a modified Lieber-DeCarli diet to mice for 28 days resulted in a significant elevation of blood alcohol content (Table 1). Mice fed control corn oil-based high fat diet exhibited no signs of liver damage (Figure 1A), or change in clinical chemistry parameters (Table 1). Conversely, treatment with alcohol-containing corn oil-based high fat modified Lieber-DeCarli liquid diet for 28 days caused fatty liver, inflammation and necrosis (Figure 1B), as well as significant elevation in enzyme markers of liver injury (Table 1). Specifically, alcohol-fed mice developed substantial liver steatosis, as evidenced by the significant elevation in oil red O-positive fat deposits (Figures 1C and D, Table 1). In addition, liver necrosis and inflammation were also observed in alcohol-treated mice as demonstrated by significant increases in necrosis, steatosis and total histology scores and a 5-fold elevation in serum activity of alanine aminotransferase (Table 1). In addition, alcohol feeding caused a significant decrease in liver glycogen content as measured by periodic acid-Schiff staining (Figures 1E and F, Table 1), and an increase in lipid peroxidation as evidenced by accumulation of 4-hydroxynonenal in liver parenchymal cells (Figure 1G and H).

Urine was analyzed for creatinine and osmolarity (Table 1). While alcohol feeding had no effect on creatinine levels, a significant increase in osmolarity, suggestive of dehydration, was observed. Collectively, these data establish that feeding corn oil-based high fat Lieber-DeCarli liquid diet may serve as an acceptable alternative to the enteral feeding mouse model for studies on alcohol-induced liver injury as it produces a similar phenotype of steatohepatitis that is much more pronounced than with a standard Lieber-DeCarli protocol.

Metabolomic analysis of alcohol-induced liver injury

Aqueous extracts of liver tissue and urine were analyzed by NMR to determine what changes in metabolome are associated with a deleterious effect of alcohol on liver. Figure 2 shows representative chromatograms from the NMR-based analysis of the urine (Figure 2A and B) and liver (Figure 2C and D) extracts. Orthogonal partial least squares model-based analysis of the data was performed to determine the metabolites responsible for the separation of the control and alcohol-treated groups. From these models, rank ordered lists of the most influential spectral bins were generated. Table 2 lists the metabolites present in those bins along with their coefficients. The magnitude of the coefficient value is proportional to its influence on the separation and the sign indicates whether that metabolite is up (+) or down (-) in alcohol-treated mice. Collectively, NMR analysis identified nine molecules in the aqueous phase of liver extracts and eleven molecules in the urine as significantly altered due to the alcohol treatment.

Principal component analysis of the NMR-derived metabolomic data shows a clear separation between control and alcohol treatments in both urine samples (Figure 3A) and liver extracts

(Figure 3B), even though alcohol and ethyl glucuronide peaks were removed from this analysis. The first principal component accounted for over 90% of the variation in the data for both the urine and liver extracts. No time-related differences in the urine metabolome were evident between samples collected from mice after 22, 30, or 36 days of alcohol feeding (data not shown). In the liver, no differences were observed between high fat-containing diet fed mice and a naïve mouse, but alcohol treatment produced a clear divergence in the metabolite profiles.

Additional analysis of the metabolites present in the organic phase of the liver metabolite extracts from control and alcohol-treated mice was performed using ESI/FTICR-MS in positive ion mode. Internal standards were employed for mass calibration and to facilitate metabolite identification based on accurate metabolite masses within <1 ppm. More than 300 metabolite features were reproducibly detected between samples within either control or alcohol groups at a signal to noise ratio above 3. Figure 4 shows a representative 280 to 330 m/z window from the analysis (from a full range of 100 to 1000 m/z) of high-fat control (Figure 4A) and alcohol-treated (Figure 4B) liver samples. High overall reproducibility between samples is evidenced by the fact that individual peaks are super-imposed between spectra from the biological replicates within each group. A zoom-in view of the 309.22 to 309.32 m/z range (Figure 4C) shows an example of several metabolites that exhibit a difference in abundance between treatments. The representative peak identified as 11, 14-eicosandienoic acid, a prostaglandin H endoperoxide synthase substrate (Koshkin and Dunford, 1998), is increased as a result of sub-chronic treatment with alcohol.

To identify the metabolites identified as changing in response to sub-chronic administration of alcohol, the Human Metabolome database and Metlin metabolome database were queried after the molecular formulae (incorporating the designated numbers of C, H, N, O, S, P, Na and K) for each peak were generated based on measured mass within 1 ppm accuracy. Table 3 lists 14 metabolites (<600 Da) identified through this process (in some cases more than one likely candidate molecules were assigned due to structural isomers of their completely identical masses).

Discussion

Rodent models of alcohol induced liver injury: state of the art and current gaps

Establishment of a compelling and human-relevant model of alcohol-induced liver injury in rodents has been difficult for a number of reasons, especially since the metabolic rates vary dramatically among species. Two major routes taken by the investigators in this field have been a survival surgery-requiring intragastric model (Tsukamoto et al., 1984), and a liquid diet-based voluntary feeding model (Lieber and DeCarli, 1982). The ability to reproduce the phenotypic hallmarks of alcohol-induced liver disease in humans, at least steatosis, inflammation, and necrosis, is usually used as a benchmark for model's success. Significantly, this report details a straightforward approach to achieve appreciable alcohol-induced liver injury in the mouse without surgery or continuous force-feeding of alcohol.

Many attempts to induce liver injury in the mouse by feeding liquid diets have not succeeded in inducing hepatitis in addition to fatty liver. When a low fat (10%) formulation of the Lieber-DeCarli liquid diet containing cocoa butter and safflower oil was fed to mice for 4 weeks, an increase in serum fatty acids, triglycerides and products of ketogenesis, along with histological changes in steatosis, were observed (Fischer et al., 2003). Similarly, when alcohol dehydrogenase-positive and -negative deer mice were fed a high mixed fat (35%; olive, safflower and corn oil) Lieber-DeCarli diet for 8.5 weeks, no statistically significant elevation in serum ALT levels or steatosis in alcohol dehydrogenase-positive deer mice was observed even though ALT levels were increased two-fold in alcohol dehydrogenase-negative deer mice (Bhopale et al., 2006). A recent study which examined the role of methionine and choline

deficiency in alcohol-induced liver disease reported that liver injury was observed after 6 weeks of feeding, but only with a modified Lieber-DeCarli formulation deficient in methionine and choline (Gyamfi et al., 2008). In female C57Bl/6J mice fed with a low fat formulation of Lieber-DeCarli diet (12% olive, safflower and corn oil) for about 7 weeks, an increase in serum markers of liver injury and advanced degree of steatosis, but not an increase in inflammation and necrosis were observed (Donohue, Jr. et al., 2007).

Our study achieved blood alcohol levels at sacrifice nearly as high as those observed previously in the liquid diet feeding studies; however, liver injury was much greater and achieved sooner than previously reported in the literature. Both liver pathology scores and serum enzyme levels were significantly elevated and were nearly identical to those reported when C57Bl/6J mice were fed corn oil-based diet intragastrically (Kono et al., 2000). Thus, we argue that the use of corn oil as the source of fat in Lieber-DeCarli formulations, similar to the previous reports on feeding high corn oil-based alcohol-containing diets to rats (Enomoto et al., 1999), or to the data from the intragastric model (Nanji et al., 1989), is the main contributing factor which greatly facilitates liver injury due to alcohol.

Metabolomic analyses delineate alcohol-induced changes in liver metabolism

Effects on energy supply—While metabolic markers in liver are not routinely available from humans, the animal model used in this study offers the opportunity to assess biochemical perturbations that affect rates of metabolism due to ingestion of alcohol. It has been well documented that both short- and long-term alcohol treatments cause acceleration (i.e., adaptive increase) of rates of alcohol metabolism *in vivo* in the rat (Bleyman and Thurman, 1979). In the mouse, it has been reported that short-term (4 hours) exposure to vaporous alcohol can also cause a significant increase in liver metabolism (Thurman et al., 1982); however, limited work has been conducted to assess the effects of long-term exposures to alcohol on rates of metabolism. In addition, basal metabolism in the mouse is much higher than in the rat or humans and these differences have not been fully characterized *in vivo*.

Treatment with alcohol is known to stimulate liver metabolism and increase oxygen uptake leading to hypoxia in the pericentral regions in the liver lobule (Ji et al., 1982). The data from our study points to two possible explanations. One metabolite found in this study, N-oleoylethanolamine, has been reported to enhance hypoxic liver injury in an ischemia reperfusion model in mice (Llacuna et al., 2006). N-oleoylethanolamine was elevated 2.6-fold after alcohol treatment and, since it is an inhibitor of ceramide metabolism thus causing high levels of ceramide and enhancing hypoxic injury, it is a very supportive piece of evidence to demonstrate metabolic links with pathological changes in liver after sub-chronic alcohol exposure. Additionally, it has been suggested that high blood levels of lactic acid correlate with hypoxia (Bakker, 1999). We also observed that lactate in liver and urine was high in alcohol-fed mice, which is consistent with data from the enteral model which demonstrated high levels of hypoxia after chronic alcohol feeding (Arteel et al., 1997). High oxygen demand in liver parenchymal cells translates into stimulation of mitochondrial function and rapid cofactor turnover, factors which exacerbate pericentral hypoxia.

Similar to previous reports in the rat, our data in the mouse shows that alcohol causes depletion in liver glycogen stores and stimulates glycolysis. Indeed, lower levels of glucose in liver of alcohol-fed mice are likely the net result of prolonged activation of glycolysis and lack of activation of gluconeogenesis. Alanine and leucine were found to be elevated in liver which is consistent with postulated alterations in glycolysis by alcohol. Furthermore, both alcohol dehydrogenase and lactate dehydrogenase require NAD⁺ and competition for this cofactor may also help to explain why lactate is high after alcohol feeding. The effects of alcohol on precursors of the TCA cycle have been characterized using the isolated perfused rat liver in the presence and absence of the added fatty acid oleate (Williamson et al., 1969). In those

studies, alcohol and oleate caused an inhibition of gluconeogenesis which is consistent with our observations. Alcohol metabolism can slow TCA cycle significantly when fatty acids are available (Williamson et al., 1969), and our data shows that similar pathways operate in the mouse. Specifically, threonine, a precursor for valine which can be metabolized to a citric acid cycle precursor succinyl CoA, was elevated in urine and liver in alcohol-treated mice. Acetate levels were also high in liver which suggests a decrease in its metabolism to acetyl CoA. Build up of these TCA cycle precursors demonstrates that energy status of the liver is lowered following alcohol treatment.

Furthermore, in a recent study that used NMR to analyze liver extracts from rats given alcohol acutely or as a binge, it was found that hepatic glucose decreased even though acetate was increased (Nicholas et al., 2008). While these observations are similar to our findings, a decrease in alanine and lactate in both acute and binge models was reported. This is in contrast to our observations in the model of sub-chronic feeding of alcohol. We argue that a high fat diet used in the sub-chronic study is the reason for these differences, since an increased supply of fatty acids may impact energy demand. This notion is supported by the fact that fatty acids reduce the supply of acetyl-CoA to the citric acid cycle (Williamson et al., 1969). Thus, we conclude that sub-chronic treatment with alcohol and high fat diet, conditions reflective of the human consumption, produces a very unique signature that could be differentiated from acute or binge models.

Fatty acid metabolism—In a model of isolated perfused rat liver, acute alcohol treatment has been shown to result in increased ketogenesis (Yuki and Thurman, 1980). In addition, lipid peroxidation, as measured by accumulation of 4-hydroxynonenal protein adducts, is known to be elevated in liver after enteral alcohol feeding in the rat (Arteel et al., 2002). Our study shows a comparable increase in lipid peroxidation in mouse liver after 28 days of alcohol feeding. This observation, together with low glucose levels detected by both NMR and FTICR-MS and elevated isoleucine and leucine found in alcohol-fed mice, suggests an increase in ketogenesis. Additionally, carnitine, which is not an essential nutrient but participates in transport of long chain fatty acids from the cytosol into the mitochondria and participates in β -oxidation, was higher in liver after alcohol treatment. It is known that carnitine is metabolized to β methyl choline and eventually to threonine which was elevated in urine after alcohol (Mitchell, 1978).

Sub-chronic treatment with alcohol causes liver inflammation as was demonstrated here and in the enteral model of alcohol-induced liver injury. Products of arachidonic acid metabolism through cyclooxygenase and lipoxygenase, such as prostaglandins, prostacyclins, thromboxanes and leukotrienes, are thought to be key mediators of alcoholic steatohepatitis. Indeed, thromboxane B₂ and leukotriene B₄ are elevated following alcohol treatment when a high fat corn oil diet is used in the enteral alcohol feeding model (Nanji et al., 1994). Acute treatment with alcohol also has been shown to increase production of prostaglandin E₂ in isolated rat Kupffer cells (Enomoto et al., 2000). In this study, linoleic acid, an essential fatty acid and a precursor of prostaglandins via arachidonic acid, was elevated in liver following sub-chronic alcohol treatment. Arachidonate was lower after alcohol which may be due to increased utilization under these conditions. In addition, our data shows that alcohol feeding caused a 2.8- fold increase in liver 7,10,13,16-docosatetraenoic acid, an arachidonate metabolite and a potent prostacyclin inhibitor (Mann et al., 1986) and a decrease in the prostacyclin metabolite 2,3- dinor-6- keto-prostaglandin F₁ α . Prostacyclins are important for regulation of platelet formation and blood clotting. In fact, 11,14-eicosadienoic acid, a substrate for prostaglandin synthetase, was elevated after alcohol which is consistent with slowed production of prostaglandin G₂ and H₂ and ultimately prostacyclins. Inhibition of platelet aggregation by an inhibitor such as 7,10,13,16-docosatetraenoic acid, and a decrease in

eicosenoic acid, a marker for membrane stability in red cells, could potentially explain why chronic drinking can cause bleeding problems in humans (Schoenfeld et al., 2007).

Metabolomic biomarkers of alcohol-induced liver injury

Since the animal model of alcohol-induced liver injury developed in this study mimics human disease, we were interested in what parallels can be drawn between species. In support of the human relevance of this mouse model, important similarities were observed. It is well known that ethyl glucuronide is a marker of alcohol ingestion in both humans (Wurst et al., 1999) and rats (Nicholas et al., 2006). Similarly, we found that ethyl glucuronide is markedly increased in alcohol-fed mice. While alcohol metabolism via glucuronidation is a very minor pathway of alcohol metabolism, the half-life of this molecule in the urine is quite long and it is detectable well after alcohol can not be measured in blood (Droenner et al., 2002).

Furthermore, in a study of 186 males categorized as drinkers and smokers (Simon et al., 1996), it was shown that alcohol drinking was associated with higher levels of palmitic, myristic, palmitoleic, oleic, and adrenic fatty acids in serum. Similar changes in liver fatty acid profiles were observed in our mouse study. Importantly, in the human study, serum levels of stearic acid were low when less than 30 drinks per week were consumed, but increased significantly with heavy drinking. Thus, elevated levels of stearic acid found in the mouse may suggest that the dose of alcohol in these animal experiments was equivalent to the human consumption of more than 30 drinks per week. However, while in human alcohol abusers the levels of linoleic acid in serum were low, we found an increase in liver linoleic acid in alcohol-fed mice. These conflicting data could be due to the differences in dietary content of fat, transient levels of fatty acids in serum versus liver in these two studies, or reflect varying rates of metabolism between species.

We also observed that alcohol treatment caused a significantly higher level of urinary n-acetylglutamine and n-acetylglycine. In humans, elevation of these molecules in urine has also been reported and linked to renal tubular injury after antibiotic treatment (Racine et al., 2004), or a mutation in the aminoacylase I (EC3.5.1.14, a renal cortex enzyme which hydrolyses N-acetylated amino acids) gene (Gerlo et al., 2006). Our observations may suggest that alcohol treatment may inhibit aminoacylase I and that urinary n-acetylglutamine and n-acetylglycine could be considered as potential non-invasive biomarkers for alcohol consumption.

There is much in the literature to suggest that antioxidant pathways are activated to help protect the body when challenged by chronic exposure to chemicals. Since alcohol exposure causes oxidative stress, it is known that glutathione plays a key protective role. In this study, taurine which is synthesized from methionine and is a metabolite of glutathione pathway was lower after alcohol treatment, similar to the data reported by Shin and Linkswiler (Shin and Linkswiler, 1974). Thus, we argue that urinary taurine may be also used as a marker of oxidative stress.

It should be noted that some of the metabolites found in this study to be changed are not unique to alcohol or high-fat diet exposure. In a recent review of metabolomic data from liver and other organs after toxic chemical exposures, it was argued that several metabolite biomarkers are hallmarks of liver injury, rather than a particular treatment (London and Houck, 2004). For example, most toxicity studies report an elevation in acetate levels in liver which is in agreement with our study. While acetate is a metabolite of alcohol, it is also produced from glycerolphospholipid and pyruvate metabolism.

In summary, this study details a mouse model for early alcohol-induced liver disease which produces liver injury consistent with pathological changes seen in human patients. The

metabolomic data obtained in this study provides new important mechanistic clues about the effects of alcohol and high fat corn oil-based diet on liver metabolism and energy utilization which may be important for understanding the pathogenesis of liver injury. We propose that several of the molecules, such as urinary levels of n-acetylglutamine, n-acetylglycine and taurine, could be used as novel non-invasive markers of alcohol consumption and oxidative stress. While further work will be necessary to determine if these biomarkers correlate with liver injury in humans, this mouse model can aid in preclinical studies.

Acknowledgments

Supported by AA016258 and ES010126.

REFERENCES

- Arteel GE, Iimuro Y, Yin M, Raleigh JA, Thurman RG. Chronic enteral ethanol treatment causes hypoxia in rat liver tissue in vivo. *Hepatology* 1997;25:920–926. [PubMed: 9096598]
- Arteel GE, Uesugi T, Bevan LN, Gabele E, Wheeler MD, McKim SE, Thurman RG. Green tea extract protects against early alcohol-induced liver injury in rats. *Biol. Chem* 2002;383:663–670. [PubMed: 12033455]
- Bakker J. Blood lactate levels. *Current Opinion in Critical Care* 1999;5:234–238.
- Bhopale KK, Wu H, Boor PJ, Popov VL, Ansari GA, Kaphalia BS. Metabolic basis of ethanol-induced hepatic and pancreatic injury in hepatic alcohol dehydrogenase deficient deer mice. *Alcohol* 2006;39:179–188. [PubMed: 17127137]
- Bleyman MA, Thurman RG. Comparison of acute and chronic ethanol administration on rates of ethanol elimination in the rat in vivo. *Biochem. Pharmacol* 1979;28:2027–2030. [PubMed: 573123]
- Bradford BU, Kono H, Isayama F, Kosyk O, Wheeler MD, Akiyama TE, Bleye L, Krausz KW, Gonzalez FJ, Koop DR, Rusyn I. Cytochrome P450 CYP2E1, but not nicotinamide adenine dinucleotide phosphate oxidase, is required for ethanol-induced oxidative DNA damage in rodent liver. *Hepatology* 2005;41:336–344. [PubMed: 15660387]
- Donohue TM, Curry-McCoy TV, Nanji AA, Kharbanda KK, Osna NA, Radio SJ, Todero SL, White RL, Casey CA. Lysosomal Leakage and Lack of Adaptation of Hepatoprotective Enzyme Contribute to Enhanced Susceptibility to Ethanol-Induced Liver Injury in Female Rats. *Alcohol Clin Exp Res*. 2007
- Donohue TM Jr. Curry-McCoy TV, Todero SL, White RL, Kharbanda KK, Nanji AA, Osna NA. L-Buthionine (S,R) sulfoximine depletes hepatic glutathione but protects against ethanol-induced liver injury. *Alcohol Clin Exp Res* 2007;31:1053–1060. [PubMed: 17428293]
- Droenner P, Schmitt G, Aderjan R, Zimmer H. A kinetic model describing the pharmacokinetics of ethyl glucuronide in humans. *Forensic Sci Int* 2002;126:24–29. [PubMed: 11955827]
- Enomoto N, Ikejima K, Yamashina S, Enomoto A, Nishiura T, Nishimura T, Brenner DA, Schemmer P, Bradford BU, Rivera CA, Zhong Z, Thurman RG. Kupffer cell-derived prostaglandin E(2) is involved in alcohol-induced fat accumulation in rat liver. *Am. J. Physiol Gastrointest. Liver Physiol* 2007;279:G100–G106. [PubMed: 10898751]
- Enomoto N, Yamashina S, Kono H, Schemmer P, Rivera CA, Enomoto A, Nishiura T, Nishimura T, Brenner DA, Thurman RG. Development of a new, simple rat model of early alcohol-induced liver injury based on sensitization of Kupffer cells. *Hepatology* 1999;29:1680–1689. [PubMed: 10347108]
- Fischer M, You M, Matsumoto M, Crabb DW. Peroxisome proliferator-activated receptor alpha (PPARalpha) agonist treatment reverses PPARalpha dysfunction and abnormalities in hepatic lipid metabolism in ethanol-fed mice. *J Biol Chem* 2003;278:27997–28004. [PubMed: 12791698]
- Gerlo E, Van Coster R, Lissens W, Winckelmans G, De Meirleir L, Wevers R. Gas chromatographic-mass spectrometric analysis of N-acetylated amino acids: the first case of aminoacylase I deficiency. *Anal Chim. Acta* 2006;571:191–199. [PubMed: 17723438]
- Gyamfi MA, Damjanov I, French S, Wan YJ. The pathogenesis of ethanol versus methionine and choline deficient diet-induced liver injury. *Biochem Pharmacol* 2008;75:981–995. [PubMed: 18036573]
- Isayama F, Froh M, Bradford BU, McKim SE, Kadiiska MB, Connor HD, Mason RP, Koop DR, Wheeler MD, Arteel GE. The CYP inhibitor 1-aminobenzotriazole does not prevent oxidative stress associated

with alcohol-induced liver injury in rats and mice. *Free Radic. Biol. Med* 2003;35:1568–1581. [PubMed: 14680680]

- Ji S, Lemasters JJ, Christenson V, Thurman RG. Periportal and pericentral pyridine nucleotide fluorescence from the surface of the perfused liver: evaluation of the hypothesis that chronic treatment with ethanol produces pericentral hypoxia. *Proc. Natl. Acad Sci U. S. A* 1982;79:5415–5419. [PubMed: 6957871]
- Kono H, Bradford BU, Yin M, Sulik KK, Koop DR, Peters JM, Gonzalez FJ, McDonald T, Dikalova A, Kadiiska MB, Mason RP, Thurman RG. CYP2E1 is not involved in early alcohol-induced liver injury. *Am. J. Physiol* 1999;277:G1259–G1267. [PubMed: 10600824]
- Kono H, Rusyn I, Yin M, Gabele E, Yamashina S, Dikalova A, Kadiiska MB, Connor HD, Mason RP, Segal BH, Bradford BU, Holland SM, Thurman RG. NADPH oxidase-derived free radicals are key oxidants in alcohol-induced liver disease. *J. Clin. Invest* 2000;106:867–872. [PubMed: 11018074]
- Koshkin V, Dunford HB. Reaction of prostaglandin endoperoxide synthase with cis, cis-eicosa- 11,14-dienoic acid. *J Biol Chem* 1988;273:6046–6049. [PubMed: 9497320]
- Lieber CS, DeCarli LM. The feeding of alcohol in liquid diets: two decades of applications and 1982 update. *Alcohol Clin. Exp. Res* 1982;6:523–531. [PubMed: 6758624]
- Llacuna L, Mari M, Garcia-Ruiz C, Fernandez-Checa JC, Morales A. Critical role of acidic sphingomyelinase in murine hepatic ischemia-reperfusion injury. *Hepatology* 2006;44:561–572. [PubMed: 16941686]
- London, RE.; Houck, DR. Introduction to Metabolomics and Metabolomic Profiling. In: Hamadeh, HK.; Afshari, CA., editors. *Toxicogenomics Principles and Applications*. Hoboken, NJ: John Wiley & Sons; 2004. p. 299-340.
- Mann CJ, Kaduce TL, Figard PH, Spector AA. Docosatetraenoic acid in endothelial cells: formation, retroconversion to arachidonic acid, and effect on prostacyclin production. *Arch Biochem Biophys* 1986;244:813–823. [PubMed: 3080955]
- Mitchell ME. Carnitine metabolism in human subjects. I. Normal metabolism. *Am J Clin Nutr* 1978;31:293–306. [PubMed: 341684]
- Nanji AA, Mendenhall CL, French SW. Beef fat prevents alcoholic liver disease in the rat. *Alcohol Clin. Exp. Res* 1989;13:15–19. [PubMed: 2646971]
- Nanji AA, Sadrzadeh SM, Thomas P, Yamanaka T. Eicosanoid profile and evidence for endotoxin tolerance in chronic ethanol-fed rats. *Life Sci* 1994;55:611–620. [PubMed: 8046997]
- Nicholas PC, Kim D, Crews FT, Macdonald JM. (1)H NMR-based metabolomic analysis of liver, serum and brain following ethanol administration in rats. *Chem Res Toxicol* 2008;21:408–420. [PubMed: 18095657]
- Nicholas PC, Kim D, Crews FT, Macdonald JM. Proton nuclear magnetic resonance spectroscopic determination of ethanol-induced formation of ethyl glucuronide in liver. *Anal Biochem* 2006;358:185–191. [PubMed: 17027904]
- Purohit V, Brenner DA. Mechanisms of alcohol-induced hepatic fibrosis: a summary of the Ron Thurman Symposium. *Hepatology* 2006;43:872–878. [PubMed: 16502397]
- Purohit V, Khalsa J, Serrano J. Mechanisms of alcohol-associated cancers: introduction and summary of the symposium. *Alcohol* 2005;35:155–160. [PubMed: 16054976]
- Racine SX, Le Toumelin P, Adnet F, Cohen Y, Cupa M, Hantz E, Le Moyec L. N-acetyl functions and acetate detected by nuclear magnetic resonance spectroscopy of urine to detect renal dysfunction following aminoglycoside and/or glycopeptide antibiotic therapy. *Nephron Physiol* 2004;97:53–57.
- Ronis MJ, Lumpkin CK, Ingelman-Sundberg M, Badger TM. Effects of short-term ethanol and nutrition on the hepatic microsomal monooxygenase system in a model utilizing total enteral nutrition in the rat. *Alcohol Clin Exp Res* 1991;15:693–699. [PubMed: 1928645]
- Schoenfeld H, Von Heymann C, Lau A, Krockner D, Neuner B, Schink T, Schwenk W, Spies CD. The effect of stress-reducing, low-dose ethanol infusion on frequency of bleeding complications in long-term alcoholic patients undergoing major surgery. *Am Surg* 2007;73:192–198. [PubMed: 17305301]
- Shin HK, Linkswiler HM. Tryptophan and methionine metabolism of adult females as affected by vitamin B-6 deficiency. *J Nutr* 1974;104:1348–1355. [PubMed: 4416751]

- Sibley D, Jerrells TR. Alcohol consumption by C57BL/6 mice is associated with depletion of lymphoid cells from the gut-associated lymphoid tissues and altered resistance to oral infections with *Salmonella typhimurium*. *J. Infect. Dis* 2000;182:482–489. [PubMed: 10915079]
- Simon JA, Fong J, Bernert JT Jr, Browner WS. Relation of smoking and alcohol consumption to serum fatty acids. *Am J Epidemiol* 1996;144:325–334. [PubMed: 8712189]
- Thurman RG. II. Alcoholic liver injury involves activation of Kupffer cells by endotoxin. *Am. J. Physiol* 1998;275:G605–G611. [PubMed: 9756487]
- Thurman RG, Paschal D, Abu-Murad C, Pekkanen L, Bradford BU, Bullock K, Glassman E. Swift increase in alcohol metabolism (SIAM) in the mouse: comparison of the effect of short-term ethanol treatment on ethanol elimination in four inbred strains. *J. Pharmacol. Exp. Ther* 1982;223:45–49. [PubMed: 7120126]
- Tsukamoto H, Gaal K, French SW. Insights into the pathogenesis of alcoholic liver necrosis and fibrosis: status report. *Hepatology* 1990;12:599–608. [PubMed: 2205558]
- Tsukamoto H, Reidelberger RD, French SW, Largman C. Long-term cannulation model for blood sampling and intragastric infusion in the rat. *Am. J. Physiol* 1984;247:R595–R599. [PubMed: 6433728]
- Williamson JR, Scholz R, Browning ET, Thurman RG, Fukami MH. Metabolic effects of ethanol in perfused rat liver. *J. Biol. Chem* 1969;244:5044–5054. [PubMed: 4390471]
- Wurst FM, Kempter C, Seidl S, Alt A. Ethyl glucuronide--a marker of alcohol consumption and a relapse marker with clinical and forensic implications. *Alcohol Alcohol* 1999;34:71–77. [PubMed: 10075405]
- Yin M, Wheeler MD, Kono H, Bradford BU, Gallucci RM, Luster MI, Thurman RG. Essential role of tumor necrosis factor alpha in alcohol-induced liver injury in mice. *Gastroenterology* 1999;117:942–952. [PubMed: 10500078]
- Yuki T, Thurman RG. The swift increase in alcohol metabolism. Time course for the increase in hepatic oxygen uptake and the involvement of glycolysis. *Biochem. J* 1980;186:119–126. [PubMed: 6989357]

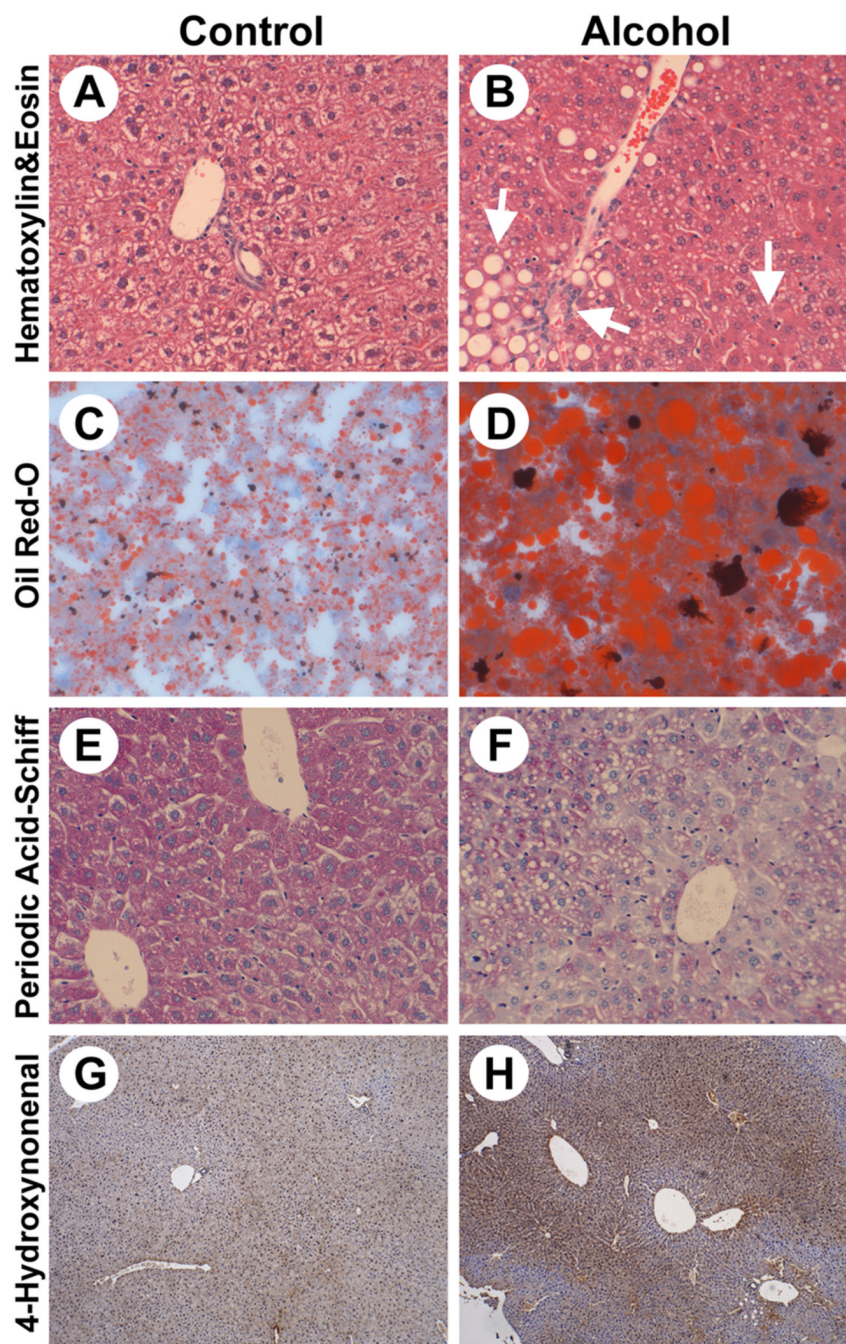


Figure 1. Feeding of the modified alcohol-containing liquid diet for 4 weeks leads to the development of steatohepatitis in the mouse. Representative liver sections from high-fat control (A, C, E, and G) and alcohol-treated (B, D, F, and H) mice are shown. Sections were stained with hematoxylin and eosin (A and B) for evaluation of liver injury, oil red-O (C and D) for quantification of fat, periodic acid-Schiff (E and F) for estimation of glycogen content, and 4-hydroxynonenal-protein adducts (G and H) for evaluation of lipid peroxidation. Magnification 200x (images A–F), or 40x (images G–H). In panel B, arrows point to the areas of steatosis, inflammation and necrosis (respectively, left to right).

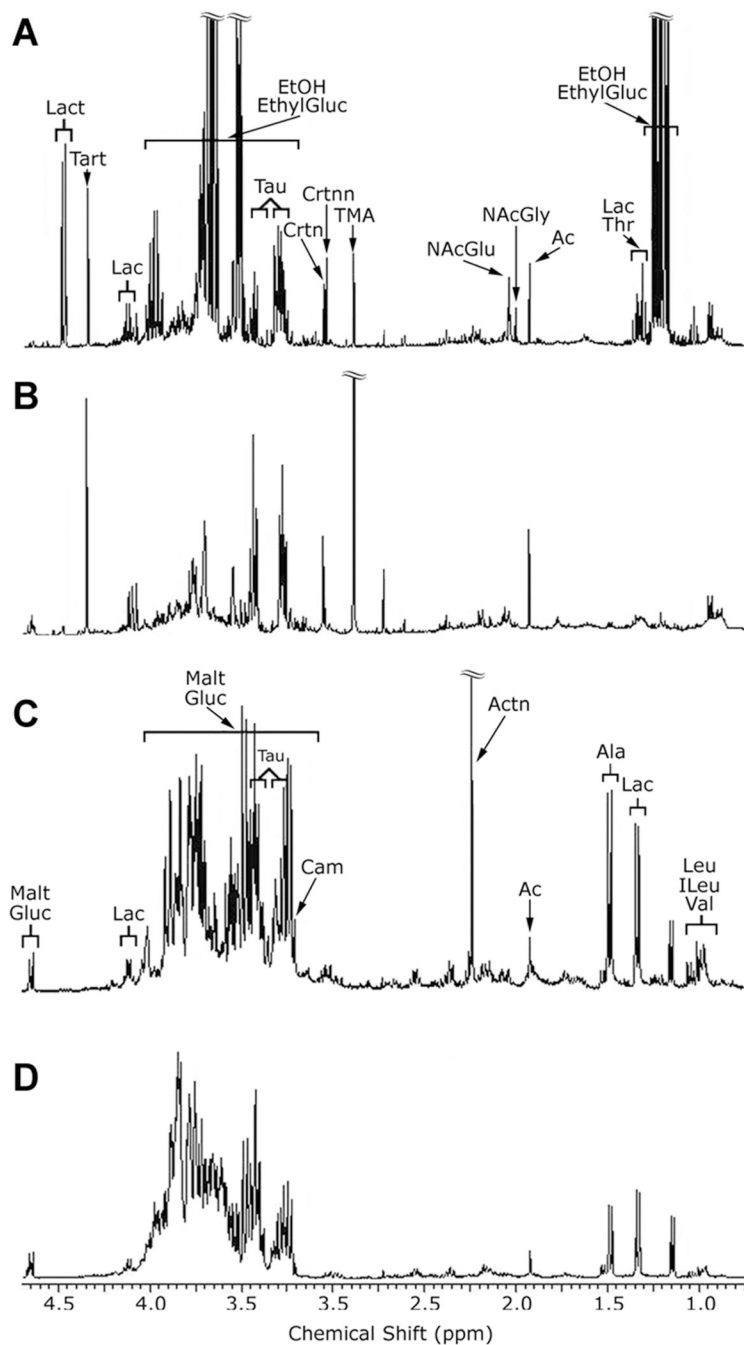


Figure 2.

¹H NMR metabolomic analysis of urine and liver reveals biochemical pathways affected by alcohol in the mouse. Representative spectra expansions of mouse urine (A and B) and liver (C and D) from control (A and C), or alcohol-treated (B and D) mice. Spectra from the alcohol-treated mice are annotated with assignments of some of the metabolites present. EthylGluc, ethylglucuronide; EtOH, alcohol; Lac, lactate; Ac, acetate; NAcGly, N-acetylglycine; NAcGlu, N-acetylglutamine; TMA, trimethylamine; Crtnn, creatinine; Crtn, creatine; Tau, taurine; Tart, tartrate; Lact, lactose; Malt, maltose; Carn, carnitine; Actn, acetone; Ala, alanine; Leu, Leucine; ILeu, isoleucine; Val, valine.

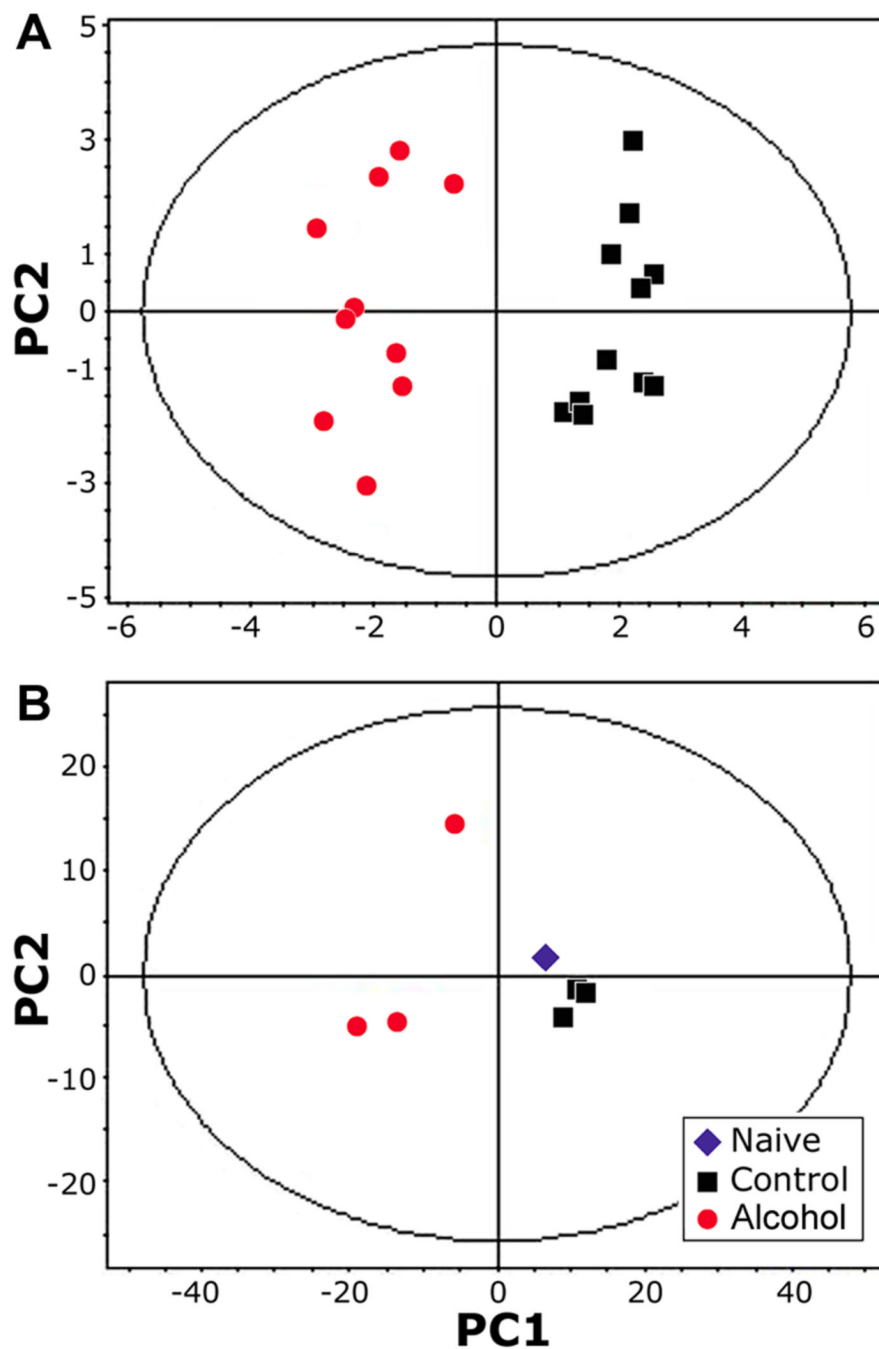


Figure 3. Principal components analysis of the ^1H NMR spectra from (A) urine ($n=4$, samples were collected on days 22, 30 and 36); and (B) liver ($n=3$ for high fat control and alcohol, samples were collected on day 28). Each point represents an individual measurement. In the urine spectra, alcohol and its main metabolite, ethyl-glucuronide, were removed from the analysis.

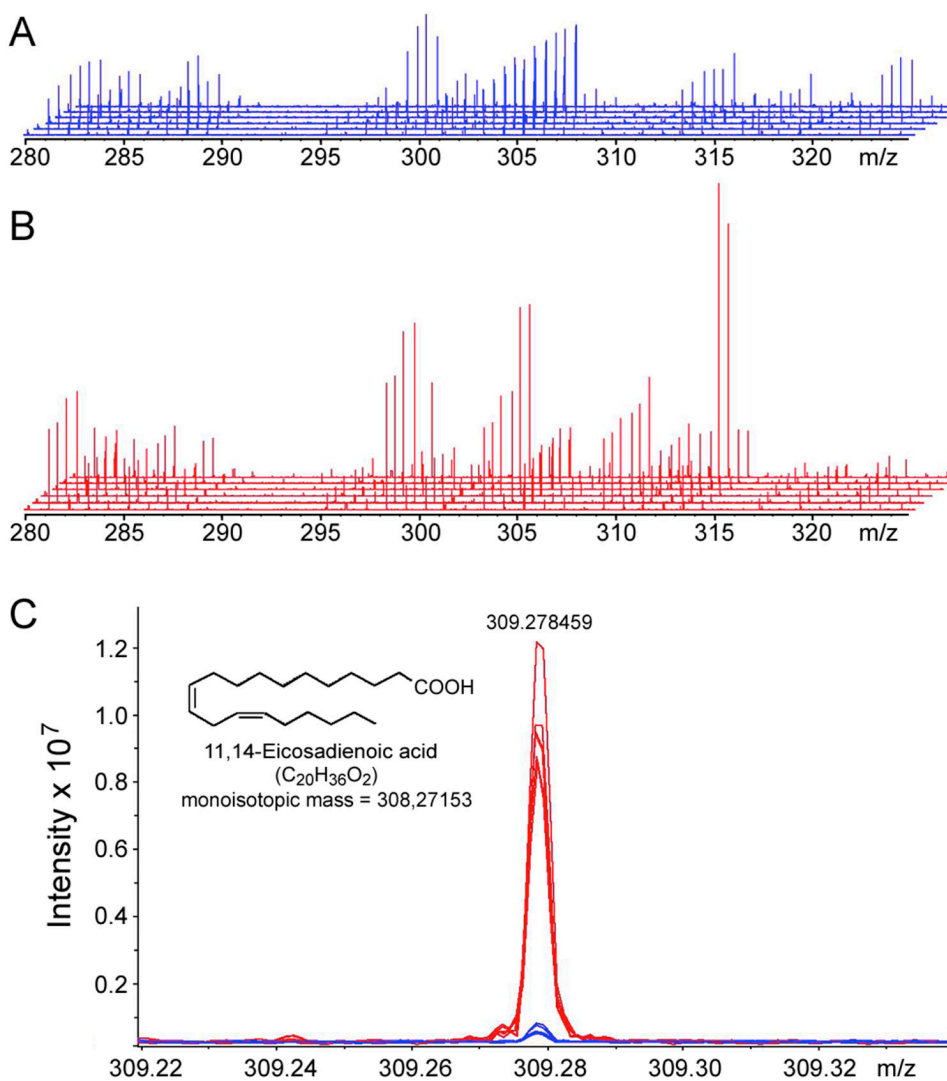


Figure 4. FTICR-MS analysis of liver metabolome identifies molecules affected by alcohol in the mouse. Expansion of the ~40 Da m/z window (from ~280 to ~330 m/z) in FTICR-MS spectra obtained from six high-fat control (A) and six alcohol-treated (B) liver samples. (C) Expansion of the m/z range from 309.22 to 309.32 showing overlaid FTICR-MS spectra from samples depicted in A and B. Four metabolites were found within this 0.10 Da window and 11, 14-eicosadienoic acid (m/z 309.278459) could be identified on the basis of accurate mass and it is elevated in liver after alcohol treatment.

Table 1

Routine clinical parameters assessed in the mouse model of the alcohol-induced liver injury.

Tissue	Measurement	Control	Alcohol
Liver	Liver/Body Ratio (%)	5.7±0.5	5.5±0.5
	Total Histology Score	0.6±0.2	4.1±0.1*
	Inflammation Score	0.5±0.6	1.4±0.8
	Necrosis Score	0.1±0.3	1.3±0.6*
	Steatosis Score	0±0	1.5±1.2*
	Oil Red-O (fat, % area)	7.3±3.6	22.9±5.5*
	Glycogen (PAS, % area)	17.5±4.3	1.4±0.6*
Serum	ALT (U/l)	15.2±3.9	74.3±18.4*
	Blood alcohol (mg/dl)	59.5±2.4	281±33*
	GGT (U/l)	5±0	5±0
Urine	Creatinine (mg/l)	18.0±1.2	18.4±0.5
	Osmolarity (mOS)	366±100	493±37*

The data shown are mean ± standard deviation (n=4).

Asterisks (*) denote statistically significant difference (P<0.05) from control group.

Table 2

Molecules identified from ¹H NMR analysis of urine and liver that differ significantly between high fat control and alcohol-treated mice.

Metabolites	Urine $R^2 = 0.96$ $Q^2 = 0.92$	Liver $R^2 = 0.96$ $Q^2 = 0.86$
Acetate		+0.0071 (0.0008)
Alanine		+0.0113 (0.0025)
Carnitine		+0.0090 (0.0021)
Dimethylamine	-0.072 (0.009)	
Glucose ^a		-0.0188 (0.0028)
Isoleucine ^b		+0.0060 (0.0006)
Lactate	+0.107 (0.028)	
Lactate		+0.0065 (0.0015)
Leucine ^b		+0.0060 (0.0006)
Maltose ^a		-0.0188 (0.0028)
N-acetyl-Glu	+0.080 (0.023)	
N-acetyl-Gly	+0.071 (0.013)	
Tartrate	-0.074 (0.014)	
Taurine	-0.121 (0.028)	
Threonine	+0.064 (0.011)	
Trimethylamine	-0.277 (0.015)	
Tyrosine	+0.043 (0.010)	
Unknown (carbohydrate)	-0.073 (0.011)	
Unknown (modified Tyrosine)	+0.097 (0.014)	
Valine ^b		+0.0060 (0.0006)

Coefficients of metabolites contributing to separation between control and alcohol treated animals in spectra of urine and liver extract. The sign indicates the direction of change as compared to controls. The values in parenthesis are the cross validated standard errors for each coefficient and confirms the statistical significance of the values.

^a & ^b The peaks for isoleucine, leucine and valine peaks fall within the same bin as do the peaks for maltose and glucose. These metabolites have the same coefficient values.

Table 3

Significant changes of liver metabolites detected by direct infusion / positive ESI-FTICR-MS between high fat control and alcohol-treated mice.

Molecule	Accurate mass by FTICR-MS	Exact Mass +/- 0.3(ppm)	Biological role	^a Fold change
Glucose, including other hexoses	180.063365	180.063388	primary energy source	0.3
2,3-dinor-6- keto-prostaglandin F1 α	326.209364	326.20932	prostacyclin metabolite	0.4
11-cis-retinaldehyde	284.214111	284.21402	vitamin A metabolite	0.4
Arachidonic acid	304.240509	304.24023	precursor of prostaglandins	0.6
2,5,7,8-tetramethyl-2-(2'-carboxyethyl)-6-hydroxychroman	278.151917	278.15182	vitamin E metabolite	0.7
Palmitic acid	256.240356	256.24023	abundant saturated fat in animal fat	1.4
Vaccenic acid or Oleic acid	282.255981	282.25589	present in animal fat	1.5
Linoleic acid	280.240356	280.24023	essential fatty acid	1.8
Stearic acid	284.271606	284.27151	from animal fats	2.6
N-oleoylethanolamine	325.29797	325.298080	ceramidase inhibitor	2.6
7,10,13,16-Docosatetraenoic acid	332.271759	332.27151	prostacyclin inhibitor	2.8
Eicosenoic acid	310.287231	310.28717	abundant in red cell membranes	9.36
3 α ,20 β -Pregnanediol	320.271522	320.271530	sterol that inhibits hepatic glucuronyl transferase	16.39
11,14-Eicosadienoic acid	308.27845	308.27153	prostaglandin H endoperoxide synthase substrate	24.11

^aRatio of the abundance of the metabolite between alcohol-treated and high fat control samples. All molecules differ significantly (P<0.05) between treatment groups. Unless otherwise noted, biological role annotations in this table were found using the Human Metabolome Database: www.hmdb.ca or Lipid Maps Database: www.lipidmaps.org/data/structure/text_search.php